

**Influence of Pb addition on the superconducting properties of polycrystalline
 $\text{Sr}_{0.6}\text{K}_{0.4}\text{Fe}_2\text{As}_2$**

Lei Wang, Yanpeng Qi, Zhiyu Zhang, Dongliang Wang, Xianping Zhang, Zhaoshun
Gao, Chao Yao, Yanwei Ma*

Key Laboratory of Applied Superconductivity, Institute of Electrical Engineering,
Chinese Academy of Sciences, P. O. Box 2703, Beijing 100190, China

Abstract

Polycrystalline $\text{Sr}_{0.6}\text{K}_{0.4}\text{Fe}_2\text{As}_2$ samples with various Pb additions (0-20 wt%) were prepared using a one-step solid state reaction. X-ray diffraction analysis shows no evidence for chemical reaction between the Pb and the FeAs-based superconductor. However, the presence of the Pb can affect the microstructure and superconducting properties of the final products. The critical transition temperature T_c indicates no degradation up to 20 wt% Pb addition, and dramatic improvements of magnetic J_c and irreversibility field H_{irr} were observed for appropriate Pb concentration. Transport critical current property of pure and Pb-added $\text{Sr}_{0.6}\text{K}_{0.4}\text{Fe}_2\text{As}_2$ tapes was also measured by a four-probe technique, and a remarkable enhancement of J_c at low fields was detected for the Pb added tapes.

* Author to whom correspondence should be addressed; E-mail: ywma@mail.iee.ac.cn

Introduction

The recent discovery of superconductivity at 26 K in the $\text{LaFeAsO}_{1-x}\text{F}_x$ compound [1] has generated tremendous interests among physicists and material scientists [2-4]. Further research has led to the discovery of superconductivity at 38 K in $\text{Ba}_{0.6}\text{K}_{0.4}\text{Fe}_2\text{As}_2$ [5]. The parent compounds, REFeAsO (1111 type, RE-rare earth) and AFe_2As_2 (122 type, A=Ba, Sr), have a quasi two-dimensional tetragonal structure, which consist of charged $(\text{LaO})^{\delta+}$ layers or $\text{A}^{\delta+}$ alternating with $(\text{FeAs})^{\delta-}$ layers. Superconductivity was produced by doping the parent compounds with electrons or holes, and the highest T_c that has been found in this FeAs-based system is around 55 K [6]. It has been accepted that these materials represent the second class of high- T_c superconductors after the discovery of cuprates in 1986 [7].

The K doped AFe_2As_2 (122 type, A=Ba, Sr) exhibits a high critical transition temperature of ~ 38 K, together with high critical current density J_c , low anisotropy, and high critical fields [8-10]. On the other hand, the synthesizing temperature is relatively low ($\sim 850^\circ\text{C}$) and no oxygen is involved, compared with that of the RE-1111 series. All these would be advantages for potential applications [8-10]. Recently, transport critical current density J_c of 1.2×10^3 A/cm² at 4.2 K in self field has been observed in $\text{Sr}_{0.6}\text{K}_{0.4}\text{Fe}_2\text{As}_2$ / Ag tapes [11]. This result would give further encouragement to the development of the newly discovered FeAs-based superconductors for potential high current applications.

Generally, chemical addition usually plays an important role in enhancing superconducting properties, by promoting the crystallization of the superconducting phase, catalyzing the intergranular coupling of the superconducting grains or introducing pinning centers. For example, the irreversibility field H_{irr} can be largely increased by C addition in MgB_2 , and a J_c enhancement was observed in Ag added YBCO [12-14]. Recently, we have reported that the H_{irr} and superconducting properties of the 122 phase iron-based superconductor can be significantly increased by Ag addition [11, 15]. On the other hand, it has been found that Pb addition effectively improved superconducting properties of BSCCO, because of a rearrangement of the band structure, as well as facilitating grain growth [16-17]. In

this paper, we studied the effect of Pb on the microstructure and superconducting properties of polycrystalline $\text{Sr}_{0.6}\text{K}_{0.4}\text{Fe}_2\text{As}_2$, and found that an enhancement of J_c in pnictide bulks and tapes can be achieved by Pb addition.

Experimental details

The polycrystalline $\text{Sr}_{0.6}\text{K}_{0.4}\text{Fe}_2\text{As}_2$ investigated were prepared by a one-step solid-state reaction method developed by our group [18], together with ball milling process. Sr filings, Fe powder, As and K pieces, with a ratio Sr : K : Fe : As = 0.6 : 0.4 : 2 : 2, were thoroughly ground in Ar atmosphere for more than 10 hours using ball milling method. After the ball milling, Pb were added into the raw powder, and then the mixture were ground in a mortar for half an hour. The final powders were filled and sealed into Nb tubes (OD: 8 mm, ID: 5 mm), the Nb tube was subsequently rotary swaged. The samples were sintered at 500°C for 15 hours, and then at 850-900°C for 35 hours in Ar atmosphere. Four kinds of samples with various Pb additions (0, 5, 10 and 20 wt%) were made for this study. The density of the sintered $\text{Sr}_{0.6}\text{K}_{0.4}\text{Fe}_2\text{As}_2$ sample is about 70% of the theoretical value of 5.89 g·cm⁻³. The fabrication of $\text{Sr}_{0.6}\text{K}_{0.4}\text{Fe}_2\text{As}_2$ tapes were described in previous papers [11, 18].

Phase identification was characterized by powder X-ray diffraction (XRD) analysis with Cu-K α radiation from 20 to 80°. Resistivity measurements were carried out by the standard four-probe method using a PPMS system. DC susceptibility of the $\text{Sr}_{0.6}\text{K}_{0.4}\text{Fe}_2\text{As}_2$ samples was measured using a Quantum Design SQUID. The samples were first cooled down to 5 K in zero magnetic field and then a magnetic field of 20 Oe was applied. The diamagnetic susceptibility due to the shielding current was measured during the warming process up to the temperatures well above T_c (ZFC: zero-field cooled). In a field of 20 Oe, the Meissner effect was measured during the cooling process. Rectangular specimens in the dimension of about 5×2.5×1.5 mm³ were cut from the samples, and magnetization measurements were performed with a PPMS system in fields up to 7 T. Magnetic critical current densities were calculated using Bean model $J_c=20Am/va(1-a/3b)$, taking the full sample dimensions. Microstructural observations were performed using scanning electron microscope (SEM). The transport critical currents of the pure and doped $\text{Sr}_{0.6}\text{K}_{0.4}\text{Fe}_2\text{As}_2$ tapes at

4.2 K and its magnetic dependence were evaluated at the High Field Laboratory for Superconducting Materials (HFLSM) in Sendai, Japan, by a standard four-probe resistive method, with a criterion of $1 \mu\text{V cm}^{-1}$.

Results and discussion

The powder X-ray diffraction patterns of the pure and Pb added $\text{Sr}_{0.6}\text{K}_{0.4}\text{Fe}_2\text{As}_2$ bulk samples are shown in Fig. 1. The pattern of pure sample is well indexed to $\text{Sr}_{0.6}\text{K}_{0.4}\text{Fe}_2\text{As}_2$. No obvious foreign phase was detected, ensuring that the proposed treatment was successful to obtain a single phase $\text{Sr}_{0.6}\text{K}_{0.4}\text{Fe}_2\text{As}_2$ sample. The Pb added samples consist of $\text{Sr}_{0.6}\text{K}_{0.4}\text{Fe}_2\text{As}_2$ as the major phase, however, Pb peaks were clearly detected in the Pb added samples, and a small amount of FeAs phase was also identified, particularly in the nominal 10 % and 20 % Pb added samples.

Figure 2 presents normalized resistivity versus temperature curves for $\text{Sr}_{0.6}\text{K}_{0.4}\text{Fe}_2\text{As}_2$ bulk samples with various Pb concentrations. All samples exhibit sharp resistive superconducting transition at T_c (onset) ≈ 35 K with $\Delta T_c \leq 2.5$ K. In particular, the 5 % Pb added samples show a zero transition at ~ 34 K. There is a general tendency for normalized resistivity above T_c to decrease with Pb addition, and the residual resistivity ratio $\text{RRR} = \rho(300\text{K})/\rho(40\text{K})$ for the pure and Pb added samples are 3.8 and 4.4, respectively. The resistive data suggest that the T_c was hardly affected by Pb addition

DC susceptibilities of pure and Pb added $\text{Sr}_{0.6}\text{K}_{0.4}\text{Fe}_2\text{As}_2$ bulk samples were measured, and all the results are shown in Fig. 3. The ZFC curve for pure samples indicates that the significant shielding currents appear at about 30 K, and increases as temperature decreases. However, the shielding currents for the Pb added samples occur at 35 K (Point A), which may suggest a crystallization improvement caused by Pb addition. The shielding currents for Pb were also seen at 9 K (Point B), which increase steadily with increasing the nominal Pb content. It is also found that, the meissner response for the Pb added samples is stronger than that of the pure samples, indicative of larger meissner fraction in Pb added samples.

Shown in the figure 4 are the magnetic J_c (at 5 K) vs magnetic field curves for the Pb added and pure bulks. As is evident from the figure, magnetic J_c in the entire

field region can be increased by Pb addition. A substantial improvement is obtained by increasing the Pb content up to 10 %, while upon further increasing the Pb content, the magnetic J_c decreases, because of too much non-superconducting phase existed (see Fig. 1). The J_c of 5 % Pb added samples at 5 K in self field is about 1.5×10^4 A/cm² and still remains above 1×10^3 A/cm² beyond 6.5 T, twice as high as for the pure samples. Most importantly, large J_c of about 2×10^4 A/cm² at 5 K in self field was achieved in the 10 % Pb added samples.

The J_c of pure and 5 % Pb added samples, as a function of magnetic fields at various temperatures, is given in the inset of Fig. 4. As expected, significant improvement of J_c at 10 K, 20 K and 30 K induced by Pb addition can be achieved. To our surprise, the J_c of the 5 % Pb added sample maintains $\sim 10^2$ A/cm² even at 30 K and high magnetic fields. Although a remarkably enhanced magnetic J_c was observed in Pb added samples, it is known that, two kinds of loops, intra-grain current loops and inter-grain current loops, contribute to the magnetization of the bulk sample. Thus, the improvement in magnetic J_c may originate from intra-grain current loops, or inter-grain current loops, or both of them.

Figure 5 depicts the variation of resistive transitions under various magnetic fields ($H=0, 1, 3, 5, 7$ and 9 T) for the pure and a 5 % Pb added samples. The resistive transition regions clearly broaden as the magnetic field increases, with only a small effect in the region near the onset of transitions. One striking feature here is that the zero transition of Pb added samples is much less sensitive to magnetic field than that of the pure samples. Upper critical field H_{c2} (T) (Filled squares for the pure samples, and filled circles for 5 % Pb added samples) and irreversibility field H_{irr} (T) (Open squares for the pure samples, and open circles for 5% Pb added samples) were estimated, using criteria of 90% and 10 % of normal state resistivity respectively, as shown in the inset of Fig. 5. Note that H_{c2} (T) was not significantly changed by Pb addition. Upper critical field was extrapolated to 0 K using the Werthamer-Helfand-Hohenberg (WHH) formula, $H_{c2}(0) = -0.693 T_c (dH_{c2}/dT)$. The slope dH_{c2}/dT estimated from the H - T phase diagram is about 8 for both samples. Taking $T_c = 34$ K, the upper critical field is $H_{c2}(0) = 188$ T. In contrast, the addition of

Pb produces a large enhancement of irreversibility field in $\text{Sr}_{0.6}\text{K}_{0.4}\text{Fe}_2\text{As}_2$. For instance, the H_{irr} for the pure samples is 3 T at 30 K, however, the extrapolated H_{irr} for the 5 % Pb added sample at 30 K is about 18 T, 15 T higher than that of the pure samples.

To further understand the Pb effects, the microstructure of pure and Pb added samples was studied as shown in Fig.6. As we can see, a dense structure with a grain size of about 5 μm in average diameter is observed in Pb added samples (Fig. 6b), much larger than the size of grains ($\sim 1 \mu\text{m}$) in the pure samples (Fig. 6a), indicating a substantial grain enlargement, which was supposed to occur during the sintering process by Pb vapor or liquid. EDX analysis on a large area in the Pb added samples clearly demonstrates that the product is composed of Sr, K, Fe, As and Pb elements and no other impurity element was found (Fig. 6c). In addition, SEM investigation using quadrant back scattering detector (Fig. 6d) shows small Pb particles dispersing in parent compound, with some residing between grains.

Therefore, it can be concluded that Pb addition inherently modifies grain dimension as well as accelerates growth, which may be responsible for some positive effects, such as the sharp resistive transition in 5 % Pb added samples and enhanced irreversibility field and magnetic J_c . However, heavy Pb addition results in a J_c degradation, because of more non-superconducting phases existed, which is supported by XRD analysis in the 10 % and 20% Pb added samples (see Fig.1).

In order to reveal the effect of Pb addition on the transport property, some pure and Pb added $\text{Sr}_{0.6}\text{K}_{0.4}\text{Fe}_2\text{As}_2$ tapes were made through the in-situ powder-in-tube method, and transport critical currents of the tapes were measured by using a standard dc four-probe method, as shown in Fig. 7. Clearly, the Pb added tapes show a higher J_c than the pure samples in low field region, and a highest J_c of 1100 A/cm^2 in self field was obtained by 5 wt% Pb addition. However, the J_c in high field region was not significantly increased. The preparation and details of superconducting properties of the Pb added wires and tapes will be reported elsewhere.

Although a remarkably enhanced magnetic J_c was observed in Pb added samples, it is known that, two kinds of loops, intra-grain current loops and inter-grain current

loops, contribute to the magnetization of granular superconductors. Thus, the improvement in magnetic J_c (Fig. 4) may originate from intra-grain current loops, or inter-grain current loops, or both of them. As the SEM study on microstructures (Fig. 6) reveals that Pb additions promote crystal growth, these large grains, meaning large dimensions of intra-grain loops, were supposed to contribute to the enhancement of magnetic J_c in the entire field region. In addition, the transport result (Fig.7) clearly shows that another contribution from inter-grain J_c improvement also exists.

Therefore, the improved magnetic J_c originates from both intra-grain and inter-grain currents, then the enlarged intra-grain current loops, maybe due to the grain size enlargement by Pb addition, are responsible for enhanced magnetic J_c at high fields. While for the improvement of transport J_c at low fields, further study on grain boundary is needed.

Conclusions

We have demonstrated effects of Pb additions on critical transition temperature T_c , magnetic hysteresis, upper critical field H_{c2} , irreversibility field H_{irr} , and transport J_c of polycrystalline $Sr_{0.6}K_{0.4}FeAs$. The critical transition temperature T_c showed no degradation up to 20 wt% Pb addition, and dramatic enhancements of magnetic J_c and irreversibility field H_{irr} were observed for appropriate Pb concentration. We notice that even transport J_c is not affected much at high fields, a substantial improvement is obtained at low fields by 5 wt% Pb addition.

Acknowledgements

The authors thank Profs. K. Watanabe, S. Awaji, G. Nishijima, Haihu Wen and Liye Xiao for their help and useful discussions. This work is partially supported by the Beijing Municipal Science and Technology Commission under Grant No. Z09010300820907, National ‘973’ Program (Grant No. 2006CB601004) and Natural Science Foundation of China (Grant No: 50777062 and 50802093).

References

1. Y. Kamihara, T. Watanabe, M. Hirano and H. Hosono, *J. Am. Chem. Soc.* **130**, 3296 (2008)
2. A. Yamamoto, A. A. Polyanskii, J. Jiang, F. Kametani, C. Tarantini, F. Hunte, J. Jaroszynski, E. E. Hellstrom, P. J. Lee, A. Gurevich, D. C. Larbalestier, Z. A. Ren, J. Yang, X. L. Dong, W. Lu, Z. X. Zhao, *Supercond. Sci. Technol.* **21**, 095008 (2008)
3. H. H. Wen, G. Mu, L. Fang, H. Yang, X. Y. Zhu, *EPL* **82**,17009 (2008)
4. C. Senatore, R. Flükiger, M. Cantoni, G. Wu, R. H. Liu, and X. H. Chen, *Phys. Rev. B* **78**, 054514 (2008)
5. M. Rotter, M. Tegel, D. Johrendt, *Phys. Rev. Lett.* **101**, 107006 (2008)
6. Z. A. Ren, W. Lu, J. Yang, W. Yi, X. L. Shen, Z. C. Li, G. C. Che, X. L. Dong, L. L. Sun, F. Zhou, Z. X. Zhao, *Chin. Phys. Lett.* **25**, 2215 (2008)
7. J. G. Bednorz and K. A. Muller, *Z. Phys. B* **64**, 189(1986)
8. Qi Y P, Zhang X P, Gao Z S, Zhang Z Y, Wang L, Wang D L and Ma Y W 2009 *Physica C* **469** 717
9. N. Ni, S. L. Bud'ko, A. Kreyssig, S. Nandi, G. E. Rustan, A. I. Goldman, S. Gupta, J. D. Corbett, A. Kracher, and P. C. Canfield, *Phys. Rev. B* **78**, 014507 (2008)
10. H. Q. Yuan, J. Singleton, F. F. Balakirev, S. A. Baily, G. F. Chen, J. L. Luo, N. L. Wang, *Nature* **457**, 565 (2009)
11. Wang L, Qi Y P, Wang D L, Zhang X P, Gao Z S, Zhang Z Y, Ma Y W, Awaji S, Nishijima G, and Watanabe K 2010 *Physica C* **470** 183
12. Ma Y W, Zhang X P, Nishijima G, Watanabe K, Awaji S and Bai X D 2006 *Appl. Phys. Lett.* **88** 072502
13. H. Salamati, A. A. Babaei-Brojeny and M. Safa, *Supercond. Sci. Technol.* **14**, 816 (2001)
14. Y. Zhao, C. H. Cheng and J. S. Wang, *Supercond. Sci. Technol.* **18**, S34(2005)
15. Wang L, Qi Y P, Gao Z S, Wang D L, Zhang X P and Ma Y W 2010 *Supercond.*

Sci. Technol. **23** 025027

16. N. Hudakova, V. Plechacek, P. Dordor, K. Flachbart, K. Knizek, J. Kovac and M. Reiffers, *Supercond. Sci. Technol.* **8**, 324 (1995)
17. G. K. Padam, S. N. Ekbote, D. K. Suri, B. Gogia, K. B. Ravat, B. K. Das, *Physica C* **277**, 43(1997)
18. Ma Y, Gao Z, Qi Y, Zhang X, Wang L, Zhang Z and. Wang D 2009 *Physica C* **469** 651

Captions

- Figure 1 X-ray diffraction patterns of pure and Pb added $\text{Sr}_{0.6}\text{K}_{0.4}\text{Fe}_2\text{As}_2$ samples.
- Figure 2 Normalized resistivities for pure and Pb added samples as a function of temperature. Inset: Temperature dependence of normalized resistivities near critical transition.
- Figure 3 Temperature dependence of DC susceptibility for pure and Pb added $\text{Sr}_{0.6}\text{K}_{0.4}\text{Fe}_2\text{As}_2$ samples.
- Figure 4 Variation of magnetic J_c as a function of applied field for pure and Pb added $\text{Sr}_{0.6}\text{K}_{0.4}\text{Fe}_2\text{As}_2$ bulk samples at 5 K; Inset: The magnetic J_c of pure and 5 % Pb added $\text{Sr}_{0.6}\text{K}_{0.4}\text{Fe}_2\text{As}_2$ samples at various temperatures.
- Figure 5 Temperature dependence of resistivity for pure (black squares) and 5 % Pb added (red circles) $\text{Sr}_{0.6}\text{K}_{0.4}\text{Fe}_2\text{As}_2$ samples in various fields $H=0, 1, 3, 5, 7$ and 9 T. Inset: Phase diagram of pure (black squares) and 5 % Pb added (red circles) $\text{Sr}_{0.6}\text{K}_{0.4}\text{Fe}_2\text{As}_2$ samples as determined from field dependence of critical transition.
- Figure 6 Scanning electron micrographs of pure (a) and 10 % Pb added (b) $\text{Sr}_{0.6}\text{K}_{0.4}\text{Fe}_2\text{As}_2$ samples; EDX spectrum (c) and QBSD image (d) for the 10 % Pb added samples.
- Figure 7 Transport J_c at 4.2 K as a function of applied field for pure and Pb added $\text{Sr}_{0.6}\text{K}_{0.4}\text{Fe}_2\text{As}_2$ tapes. The measurements were performed in magnetic fields parallel to the tape surface.

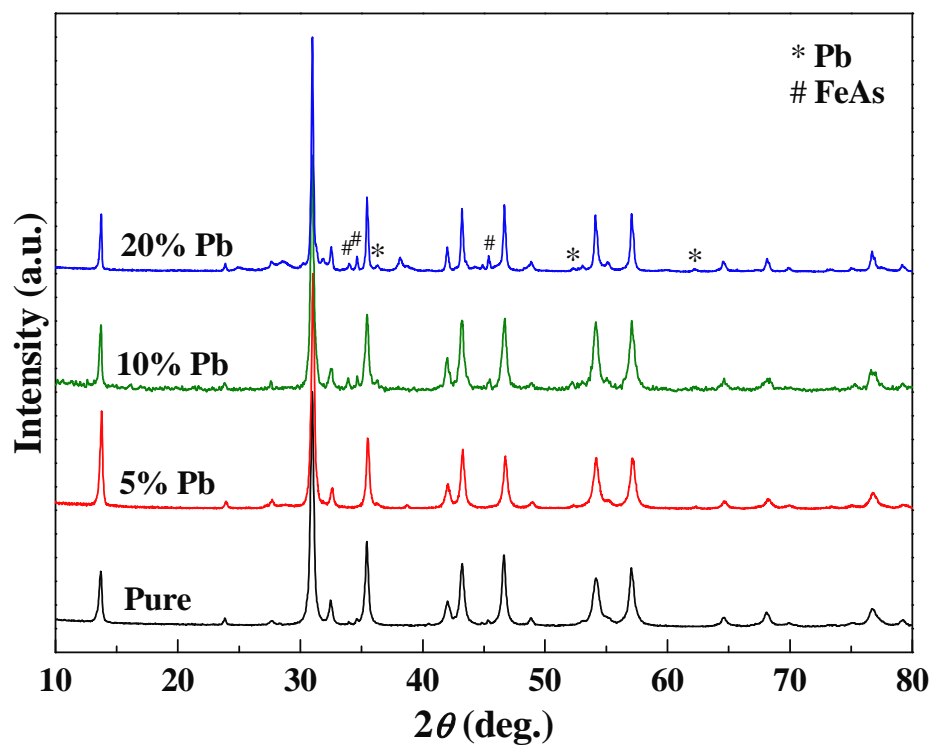


Figure 1 Wang et al.

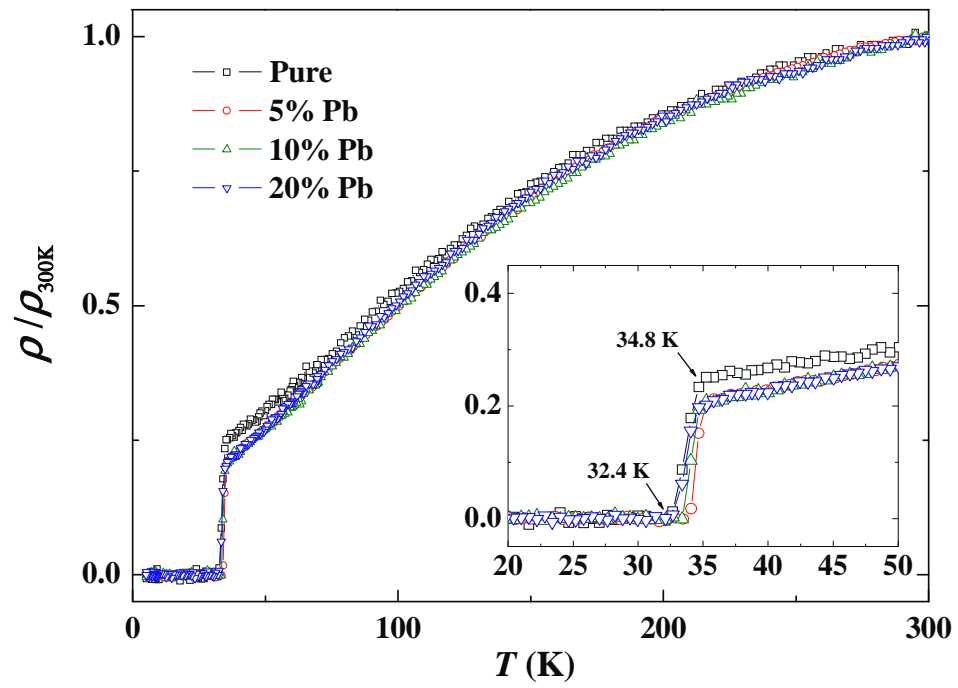


Figure 2 Wang et al.

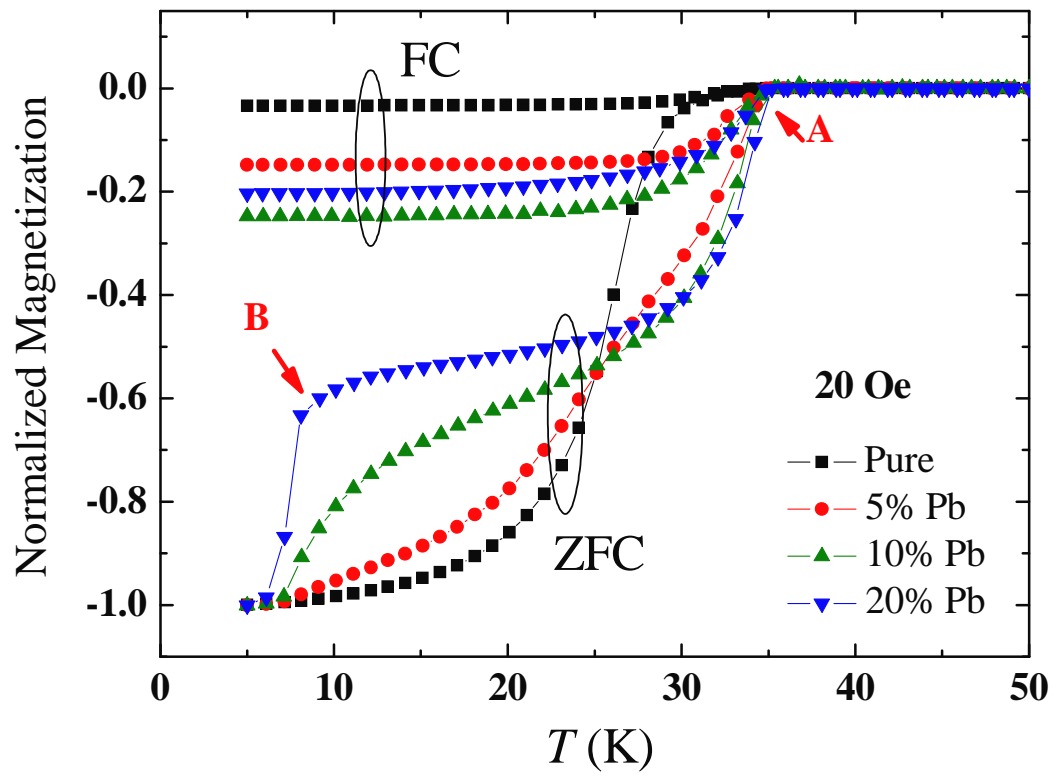


Figure 3 Wang et al.

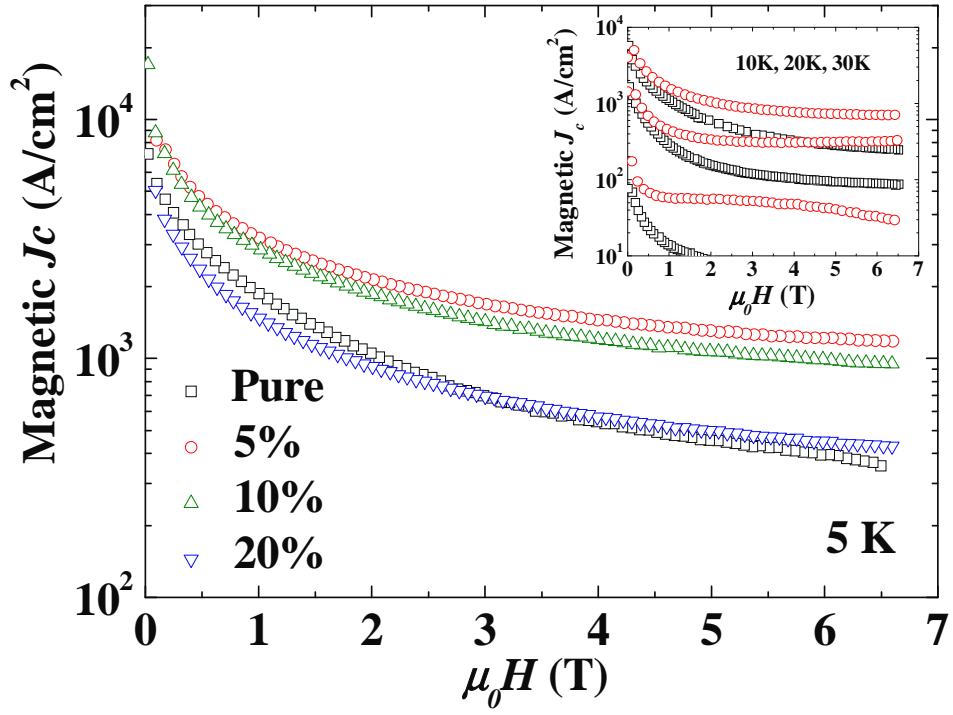


Figure 4 Wang et al.

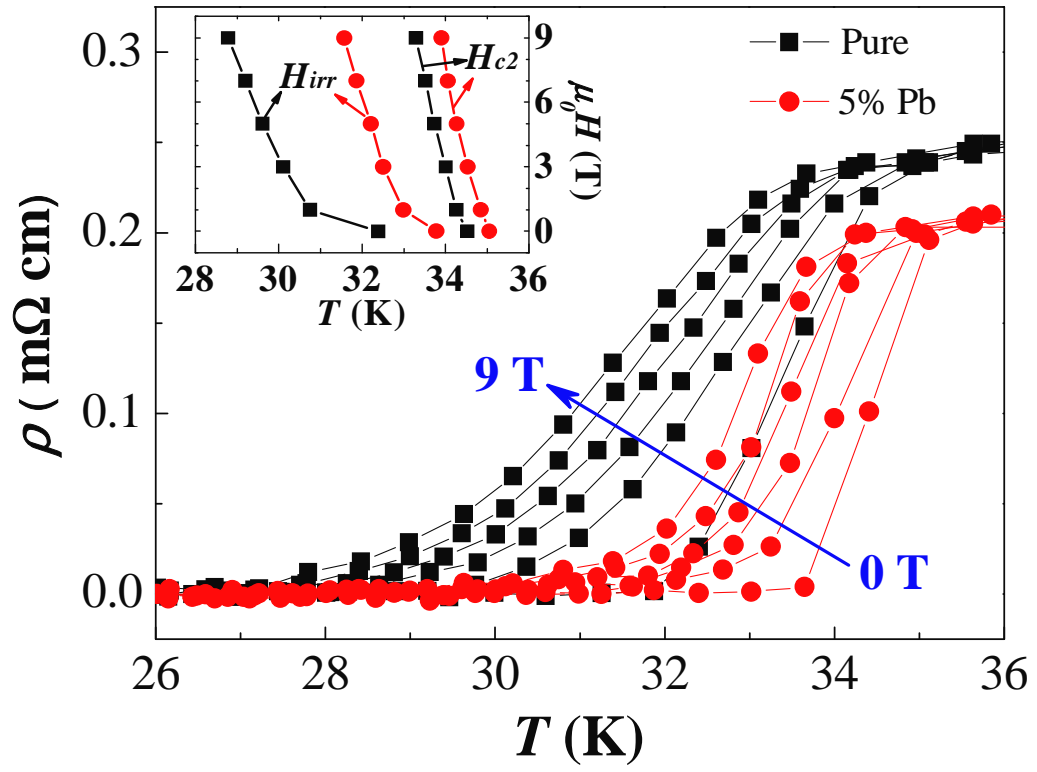


Figure 5 Wang et al.

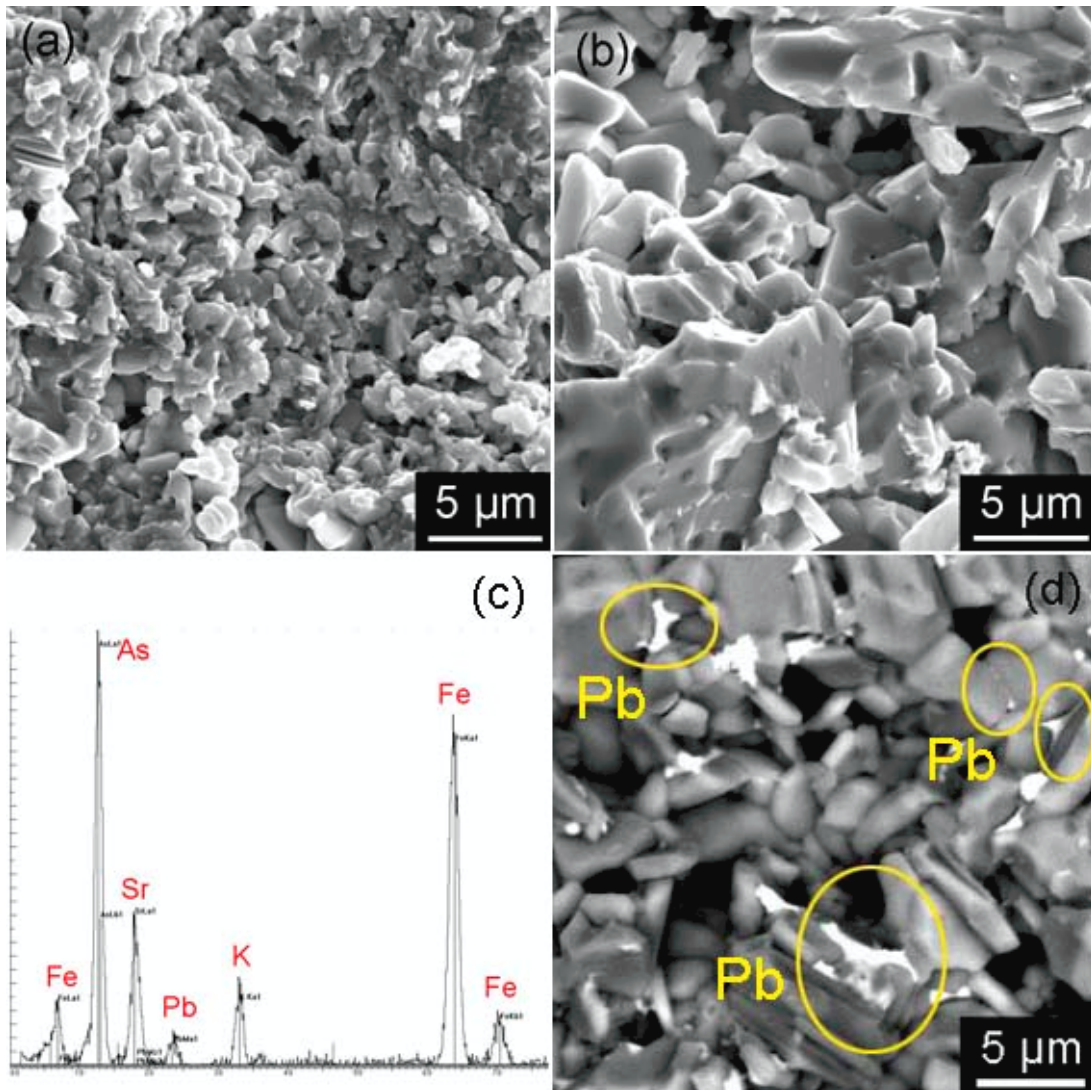


Figure 6 Wang et al.

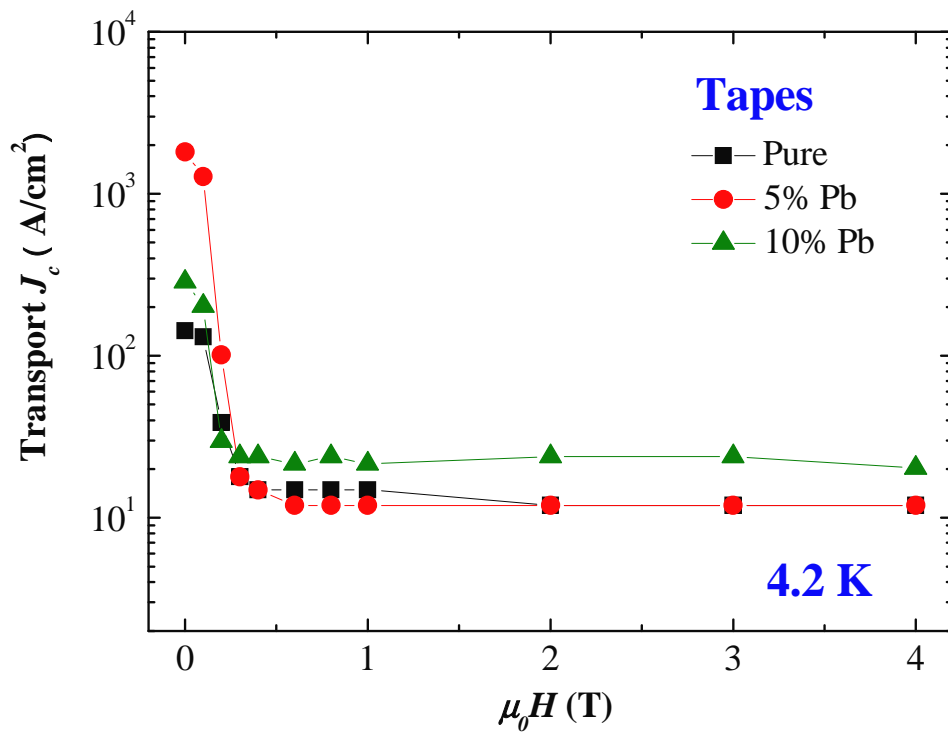


Figure 7 Wang et al.